

Evaluation of Paper Industry Wastes in Construction Material Applications

Enori Gemelli^{a*}, Nelson Heriberto Almeida Camargo^b, Janaína Brescansin^c

^{a,b}Department of Mechanical Engineering, Center of Technological Sciences

^cDepartment of Civil Engineering, Center of Technological Sciences, UDESC - Santa Catarina State University, C.P. 631, 89223-100 Joinville - SC, Brazil

Received: April 30, 2001; Revised: September 22, 2001

The influence of the application of residues from the cellulose and paper industry in construction mortar was investigated. Mortars were prepared with CPI-S-32 or CPII-Z-32 Portland cements and sand in a 1:3 proportion. Four solids residues, *i.e.*, Fiber, Dregs, Bottom Ash and Grit, were incorporated in the mortars in varying proportions. The bottom ash and dregs were used in place of cement, while fiber and grit were used to replace sand. The aging time of the samples was varied from 7 to 28 days. The results demonstrated that the type of cement and the aging time exerted a strong influence on the samples' microstructure and resistance to axial compression. The best values were obtained at 28 days of age with the CPI-S-32 cement. On the other hand, the type of residue and its concentration also affected microstructure and resistance to axial compression. The best results were obtained from bottom ash and grit.

Keywords: *wastes, mortar, building materials*

1. Introduction

A large cellulose and paper manufacturer can produce about 5000 m³ of solid wastes per month. According to the Brazilian NBR 10004 code, class II and III wastes are classified as valuable. From a practical standpoint, therefore, they can be used as sources of energy or as raw materials to produce new materials.

Recent studies¹⁻⁴ have revealed that a variety of residues can be used as raw materials in the construction industry. Depending upon their chemical composition, these wastes can be incorporated into mortars to partially replace cement and/or traditional sand, reducing the cost of mortars and improving environmental protection.

The purpose of this work was to assess the performance of mortars produced with wastes from industrial cellulose and paper processes. To this end, four types of residue, namely fibers, dregs, bottom ash and grit, were selected. The fibers, deriving from the cellulose paste washing process, and the dregs from the cellulose production process, were collected from a chemical reactor operating between 900 and 1000 °C. Bottom ash is a residue from the burning of biomass, while grit is a waste product from burnt oil

impregnated on sand, which is used as a fluidized layer to separate oil from impurities.

In this study, we produced and characterized mortars with varying amounts (in volume) of wastes. Bottom ash and dreg residues were used to partially substitute the Portland cement, and fiber and grit were used to partially replace sand. These wastes were supplied by Klabin Celucat S.A., a large cellulose and paper manufacturer.

2. Materials and Experimental

2.1. Portland cement

Portland cement, which is a product of the clinker process, consists essentially of calcium and sulfate silicates. The main compounds contained in Portland cement are CaO, SiO₂, Al₂O₃ and Fe₂O₃, although MgO, SO₃, Na₂O, K₂O and TiO₂ are also present in smaller amounts.

For this study we used CPI-S 32 and CPII-Z 32 Portland cement⁵.

2.2. Aggregate (sand)

The term "aggregate" is commonly employed in concrete technology to indicate sand, which is constituted of a mixture of particles of varying sizes⁶. The sand used in this

*e-mail: dem2eng@joinville.udesc.br

work originates from sedimentary layers formed in riverbeds. Table 1 presents the granulometric distribution of the aggregate (sand) used in this study.

2.3. Solid grit waste

This waste consists basically of silica (sand) covered by a layer of ash, and is produced by burnt oil impregnated on the sand. In this study, we used only ≤ 2 mm diameter particles (10 mm mesh) taken from this waste. Table 2 shows the granulometric analysis of this grit.

2.4. Solid bottom ash waste

The solid bottom ash waste, composed of hard agglomerates, was milled to produce raw material, using water and a porcelain ball mill at 50 rpm for 24 h. The proportion of porcelain balls and waste was 2:1 in mass. After milling, the sludge was sieved through a 100-mesh sieve and shaken in a mechanical shaker for 2 h, followed by drying for 4 h in a rotary evaporator at 70 °C (silicone oil temperature) at 8 rpm. The powder thus obtained had an average particle size of $< 0,5$ mm and humidity of approximately 6 to 7%.

2.5. Solid dreg waste

This waste was mechanically shaken (690 rpm) in water for 10 h to break up the agglomerates and homogenize the solution. Subsequently, the sludge was dried in a drying

Table 1. Particle size distribution of the aggregate, according to the NBR 77211 code⁷.

Sieve mesh size (mm)	Mass retained on the sieve (%)
2.38	0.00
2.00	0.05
1.19	0.17
0.59	8.58
0.42	29.84
0.29	61.36

Table 2. Granulometric distribution of the solid grit waste.

Sieve mesh size (mm)	Mass retained on the sieve (%)
2.38	1.77
2.00	3.73
1.19	6.64
0.59	12.89
0.42	16.25
0.29	18.22
0.149	19.70
0.074	20.80

room at 90 °C for 24 h. The dried material was black, with some yellow stains caused by the presence of Na₂S in the waste. The dried waste was passed through a 100-mesh sieve and thermally treated at 900 °C for 2 h, after which it was dispersed in methanol in a proportion of 1:2 in volume and again mechanically shaken for 3 h. The sludge was then dried in a rotary evaporator and sieved through a 100-mesh sieve.

2.6. Solid fiber waste

In order to break the solid fiber waste agglomerates, they were subjected to a 24-h ball milling process using ethical alcohol. The resulting sludge, greenish-black in color, was mechanically shaken for 2 h, dried in a rotary evaporator and sieved through a 50-mesh sieve. This dried material, consisting of short fibers, was of a uniformly pale gray color.

2.7. Production of mortar

The mortars were produced according to the Brazilian NBR 12821 code⁸. Table 3 lists the mixtures used in the preparation of the mortars. Each mixture was molded into 50 mm diameter, 100 mm long samples⁹.

2.8. Molding of the samples

The samples were molded in three mortar layers, with each layer compacted using 20 strokes of a standard rod¹⁰, and removed from the molds after 24 h. The samples were then aged in alkaline water for 28 days to achieve complete hydration of the cement. Upon completion of the aging process, the samples were subjected to mechanical axial compression tests¹¹. To this end, the samples' upper surfaces were coated with sulfur to render them flat and smooth for better contact with the mechanical compression devices¹⁰.

2.9. Microstructural and morphological characterization

The microstructure and morphology of the cement, sand and waste powders were characterized by scanning electron microscopy (SEM). After being dried in a drying room for 24 h at 100 °C, fragments of the samples obtained from the mechanical tests were also subjected to SEM analyses.

3. Results and Discussion

3.1. Axial compression strength

The mortar samples were subjected to mechanical axial compression tests at approximately 500 N/s. Tables 4, 5 and 6 illustrate the results of these tests. The samples produced only with CPI-S 32 cement were aged for 7 and 28 days, while those prepared with CPII-Z 32 cement were aged for 28 days.

Table 3. Amount of materials used to produce the mortars. * Water/cement factor. ** Water/(cement plus bottom ash/dregs) factor.

Mortars	Cement CPIS32 (g)	Sand (g)	Bottom ash (g)	Grit (g)	Dregs (g)	Fibers (g)	Water (mL)	Factor W/C
(Rs)	624	1872	0	0			300	0.48*
(A)	592.8	1872	27	0			300	0.49**
(B)	561.6	1872	54	0			300	0.48**
(C)	624	1779	0	49			300	0.49*
(D)	624	1686	0	98			300	0.49*
(E)	624	1593	0	147			300	0.49*
(F)	624	1500	0	196			300	0.49*
(G)	592.8	1872	0		16.34	0	300	0.49**
(H)	624	1779	0		0	28.25	300	0.48*
(I)	592.8	1779	0		16.34	28.25	300	0.49**
(J)	592.8	1872	27.00		0	0	300	0.49**
	Cement CPIIZ32 (g)							
(Rz)	624	1872	0	0			300	0.48*
(K)	561.6	1872	54	0			300	0.48**
(L)	624	1686	0	98			300	0.49*

Table 5 shows a comparison of the mechanical strength tests carried out on the samples with different types of residue, indicating that bottom ash produced the best results. Although the other residues showed lower performance values, their mechanical strength was comparable to that of building materials used in many applications. It can be observed that the mechanical strength depends on the aging time of the samples. The results obtained with 7 days of aging (Table 4) correspond to 50-60% of the values obtained with an aging time of 28 days (Table 5).

Another important point to be observed is the difference in mechanical strength between one type of cement and another. The mortar without residue prepared with CPII-Z-

32 cement presented low resistance (~5 MPa) compared to that produced with CPI-S-32 cement (~21 MPa). This difference is explained in the discussion of the microstructural study, below, although it is attributed mainly to the fact that the CPI-S-32 was replaced by CPII-Z-32 cement.

Our conclusions regarding axial mechanical strength are that bottom ash and grit residues stand out from the other types of waste as materials that can be used to partially substitute Portland cement and sand, respectively. The addition of these residues to mortar produced with CPII-Z-32 Portland cement caused a slight increase in mechanical strength (Table 6).

These results led us to conclude that fiber and dreg wastes are better employed as energy sources than as

Table 4. Average strength of the samples prepared with CPI-S-32 Portland cement after 7 days of aging. Amount of residue in volume (%).

Samples	Average rupture stress (MPa)
Matrix (Rs)	12.38
Cement + 5% bottom ash (A)	8.68
Cement + 10% bottom ash (B)	6.50
Cement + 5% grit (C)	7.50
Cement + 10% grit (D)	10.00
Cement + 15% grit (E)	9.53
Cement + 20% grit (F)	8.94

Table 5. Average strength of the samples prepared with CPI-S-32 Portland cement after an aging time of 28 days. Amount of waste in volume (%).

Samples	Average rupture stress (MPa)
Matrix (Rs)	21.28
Cement + 5% fibers (G)	14.45
Cement + 5% dregs (H)	16.94
Cement + 5% fibers and 5% dregs (I)	15.90
Cement + 5% bottom ash (J)	20.36

Table 6. Average strength of the samples produced with CPII-Z-32 Portland cement after 28 days of aging. Amount of waste in volume (%).

Samples	Average rupture stress (MPa)
Matrix (Rz)	4.86
Cement + 10% bottom ash (K)	5.23
Cement + 10% grit (L)	5.32

hydraulic binders. These wastes can be burned along with the primary biomass and can then be partially eliminated, increasing the amount of bottom ash. Mortar samples produced with bottom ash and grit will, therefore, be investigated more extensively by SEM metallography.

3.2. Microstructural and morphological characterization

Portland cement. Our metallographic observations revealed differences between Portland cements. Figures 1 and 2 indicate that the composition of the CPII-Z-32 cement presents a large amount of impurities in comparison to the CPI-S-32 cement. These impurities consist mainly of inert ash in the cement, represented by the smaller particles in Fig. 1. The mortar's low mechanical strength is attributed mostly to this large amount of inert ash.

Bottom ash waste. The bottom ash powder was found to have a scattered particle shape and size, as shown in Fig. 3. With regard to the morphology of the Portland cement and bottom ash powder, the latter clearly shows a smaller particle size than that of the cement. This means that the bottom ash was subjected to an excessively long milling time, *i.e.*, this residue did not require 24 h of milling, and reducing the milling time would have resulted in a morphology closer to that of the cement.

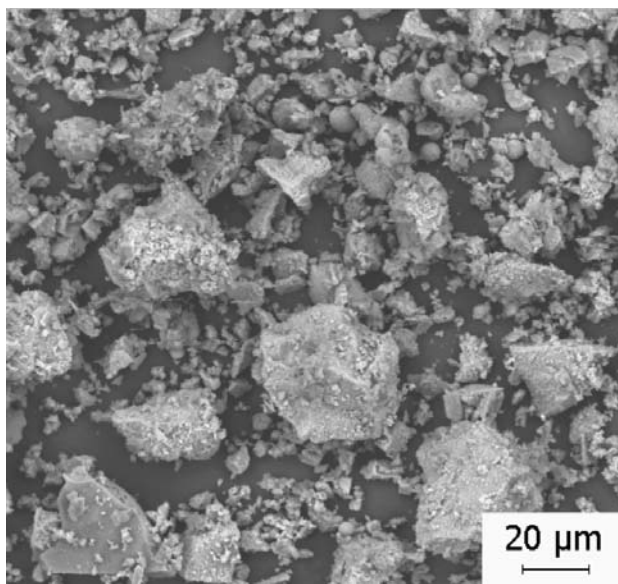


Figure 1. SEM micrograph showing the morphology and impurities, mainly inert ash, in CPII-Z 32 Portland cement powder.

Grit waste. The grit waste used as an aggregate in place of sand showed a distinctive morphology composed of grains of sand ($d < 500 \mu\text{m}$) covered by small particles of ash, as shown in Fig. 4.

Sand (aggregate). The morphological study of the sand allowed us to assess its quality, revealing that it consisted of grains ($d < 300 \mu\text{m}$) partially covered by clay (Fig. 5).

Microstructure of the samples. The microstructural characterization of the samples, after an aging time of 28 days, was carried out on the fracture cross-section; the results of this characterization are presented below.

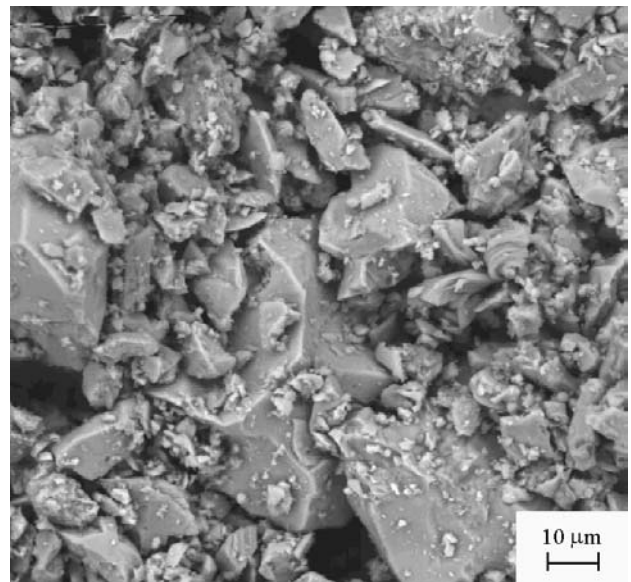


Figure 2. SEM micrograph of the morphology of CPI-S-32 Portland cement powder.

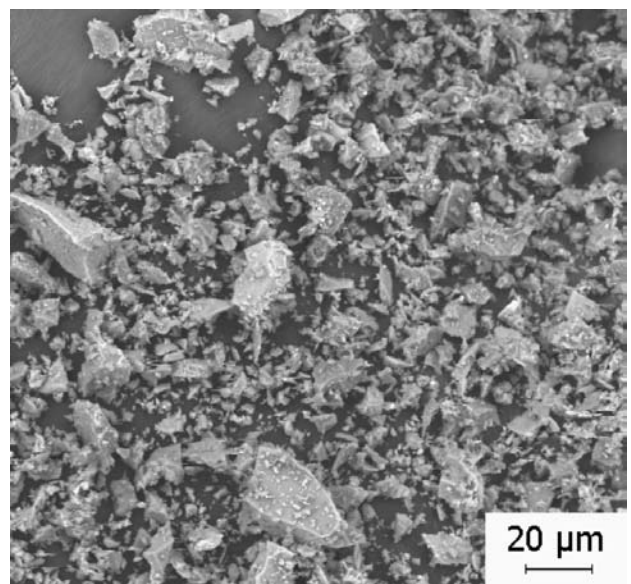


Figure 3. SEM micrograph of the morphology of bottom ash waste powder.

CPII-Z-32 cement/sand (Rz). The microstructural characterization of the CPII-Z-32 cement/sand revealed high porosity at the cement/sand interface, possibly due to the great amount of inert ash in the CPII-Z-32 cement. Inert ash inhibits the nucleation and growth of anhydrite crystals in mortar. Therefore, increased porosity caused by alkali-aggregate reaction during the formation of gel interferes in the quality of the gel/aggregate interface.

Figure 6 depicts a porous region that clearly shows poor development of the gel and anhydrite crystals in the mortar. Thus, the presence of inert ash in the cement led to a limited alkali-aggregate reaction and, hence, to high porosity and insufficient, disordered formation of anhydrite crystals.

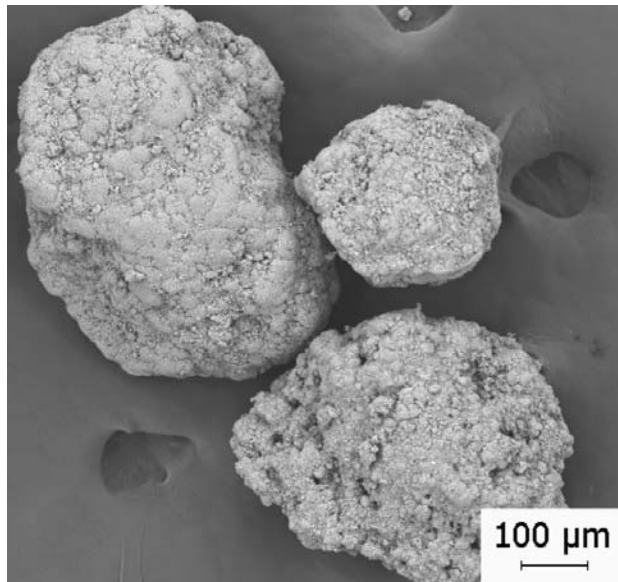


Figure 4. SEM micrograph of the morphology of the as received grit.

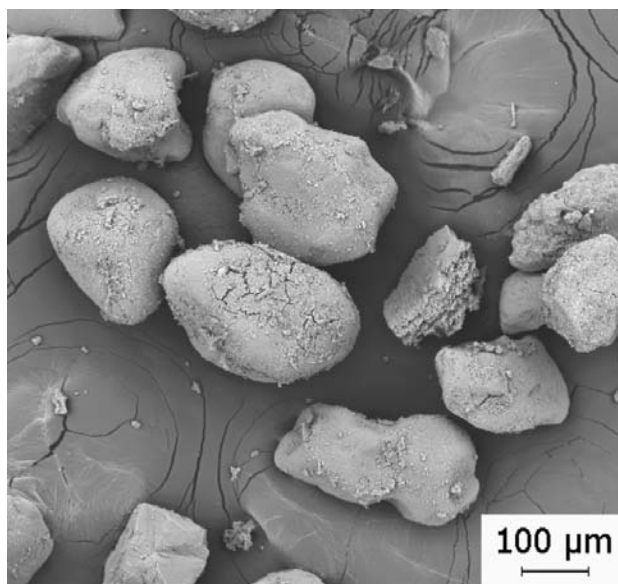


Figure 5. SEM micrograph of clay coating the sand grains.

CPI-S-32 cement/sand (Rs). In contrast to the above-mentioned CPII-Z-32 cement, the mortar produced with CPI-S-32 cement was far more homogeneous, with little porosity and well developed anhydrite crystals. Gel, resulting from the alkali-aggregate reaction, was formed between the cement paste and the sand, as illustrated in Fig. 7. The cement paste contracted at this interface due to the dehydration the samples had been subjected to in the drying room in preparation for the SEM analysis.

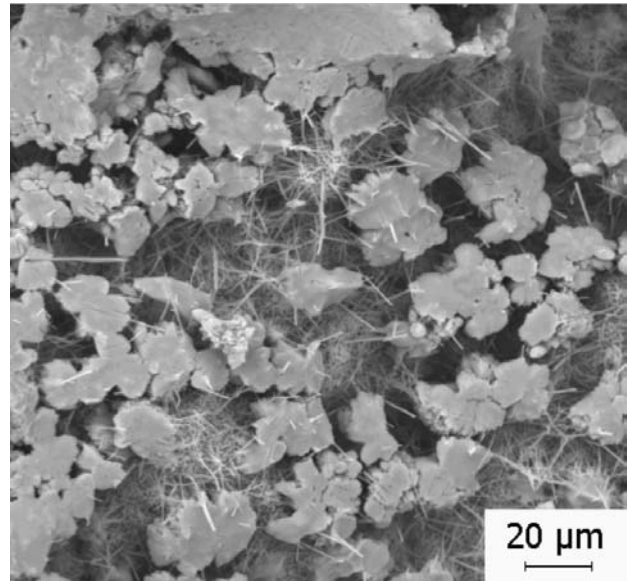


Figure 6. SEM micrograph of the porosity and disordered development of anhydrite crystals on the (Rz) Matrix (CPII-Z-32 cement/sand) after 28 days of aging.

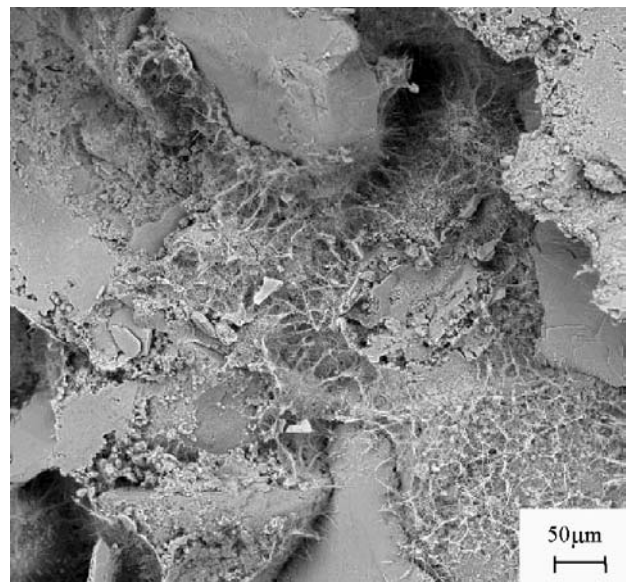


Figure 7. SEM micrograph showing gel crystallization on the (Rs) Matrix (CPI-S-32 cement/sand) after 28 days of aging.

CPII-Z-32 cement/sand with 10% bottom ash (K). Figure 8 presents a less porous microstructure than that of the matrix (cement/sand/water), indicating that the bottom ash improved the material's microstructural characteristics. A better aggregate/gel interface was thus obtained, since bottom ash works as an agglutinate in the alkali-aggregate reaction, improving the gel/aggregate interface. This explains the higher mechanical strength of this mortar (K) in comparison to the matrix (Rz). Improved nucleation and growth of anhydrite crystals in the material was also observed, with a resulting decrease in porosity and

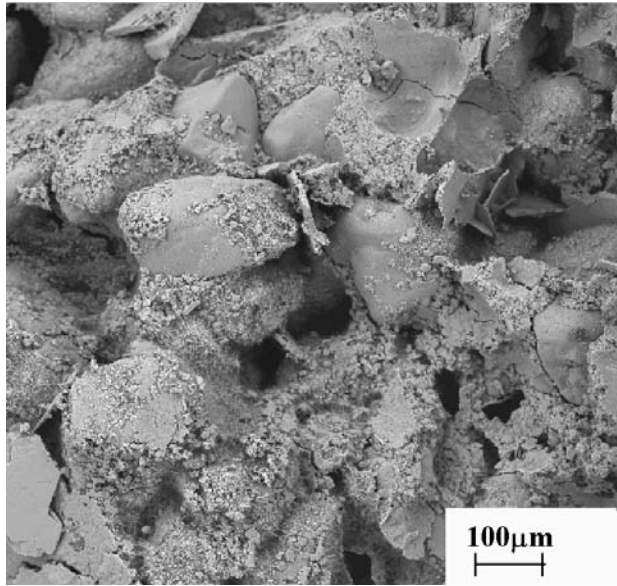


Figure 8. SEM micrograph of the porosity and aggregate/gel interface of sample (K) (CPII-Z-32 cement/10% bottom ash/sand) after 28 days of aging.

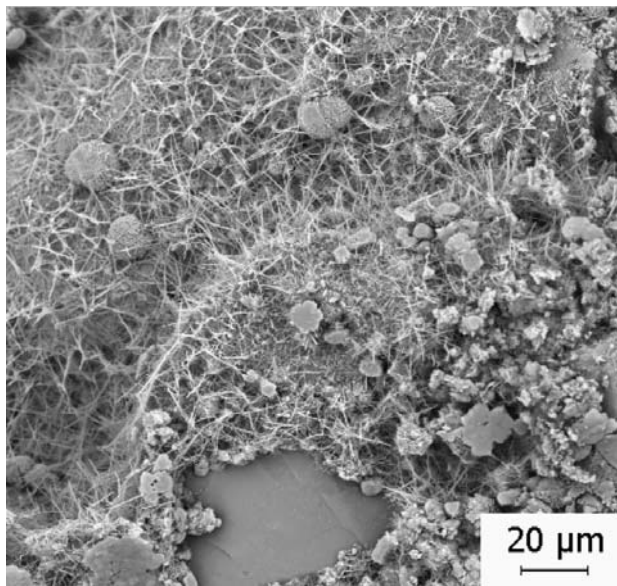


Figure 9. SEM micrograph of the anhydrite crystals in sample (K) (CPII-Z-32 cement/10% bottom ash/sand) after 28 days of aging.

a more organized development of the fibers. It was also found that the anhydrite crystals were smaller than those observed in the matrix (Fig. 9), which may have been due to water absorption by the bottom ash powder.

CPI-S-32 cement/sand with 5% bottom ash (J). Figures 10 and 11 show well-distributed incorporation of the bottom ash throughout the samples' microstructure. The bottom ash did not expand or retract the mortar during water loss and absorption, resulting in the very low formation of porosity (cavities). Crystal growth from the alkali-aggregate reaction occurred in a few random places on the

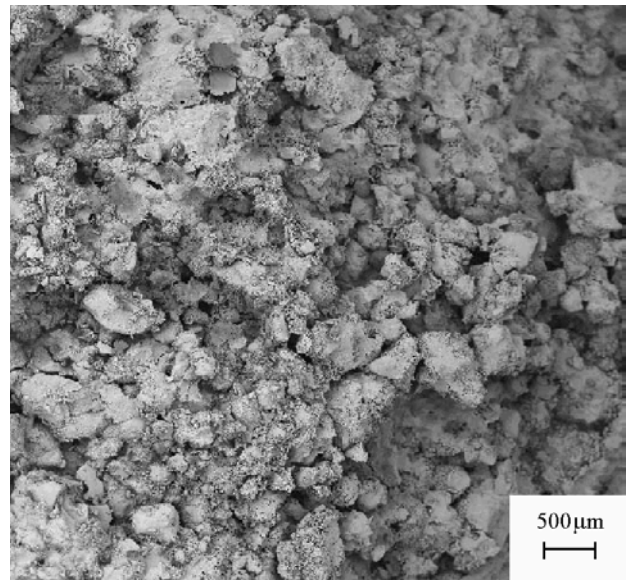


Figure 10. SEM micrograph of a general view of the (J) samples (CPI-S-32 cement/5% bottom ash/sand) after 28 days of aging.

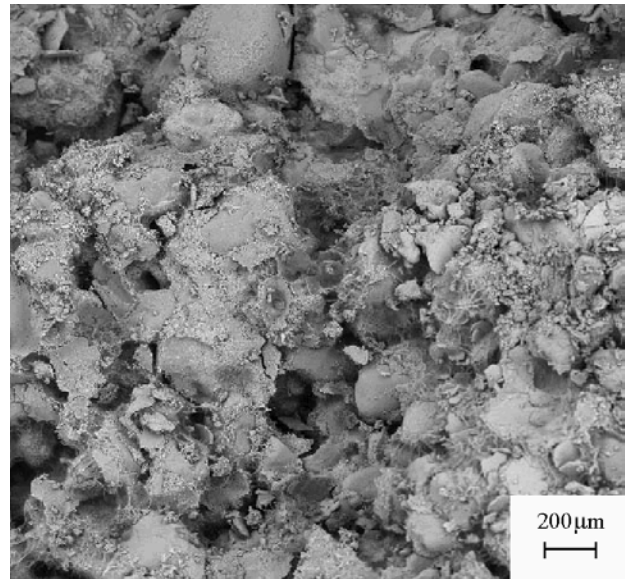


Figure 11. SEM micrograph of the aggregate partially covered by bottom ash powder in the (J) samples (CPI-S-32 cement/5% bottom ash/sand) after 28 days of aging.

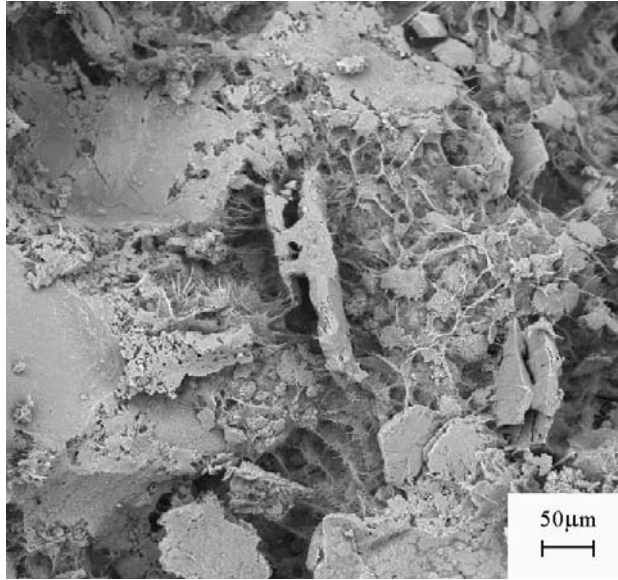


Figure 12. SEM micrograph of crystals growing on the surface of aggregates in the (J) samples (CPI-S-32 cement/5% bottom ash/sand) after 28 days of aging.

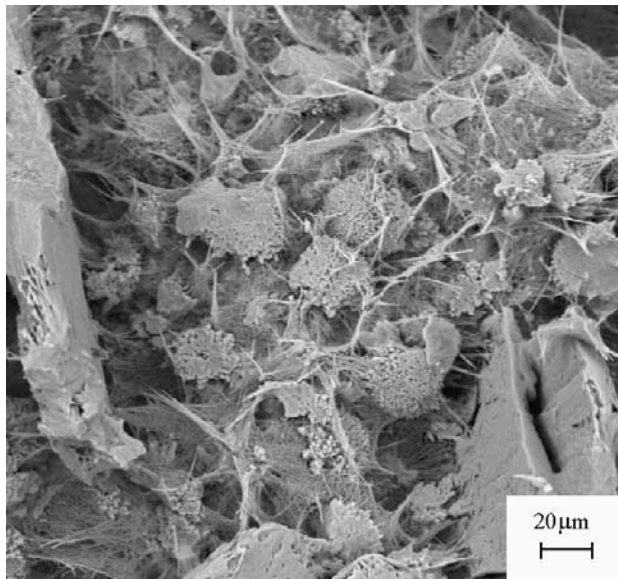


Figure 13. SEM micrograph of the aggregate/paste interface in the (J) samples (CPI-S-32 cement/5% bottom ash/sand) after 28 days of aging.

sample's surface. Nevertheless, these crystals were better developed than those in the Rs matrix (CPI-S-32 cement/sand), as illustrated in Figs. 12 and 13.

CPII-Z-32 cement/sand with 10% grit (L). The microstructural analysis of the CPII-Z-32 cement/aggregate (sand plus grit) revealed a good cement/aggregate interface (Fig. 14). Gel was found to be present in the form of small agglomerates all over the sample's fracture surface. The material also presented a disordered growth and a smaller amount of anhydrate crystals (Fig. 15), possibly due to the

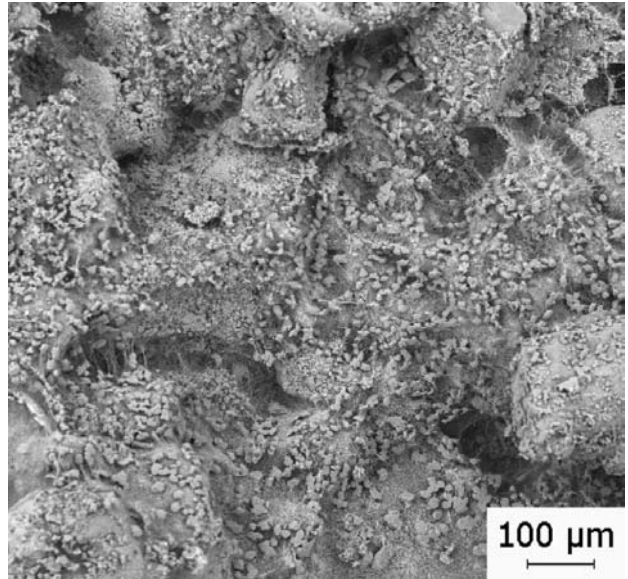


Figure 14. SEM micrograph of the aggregate/gel interface in the (L) samples (CPII-Z-32 cement/sand/5% grit) after 28 days of aging.

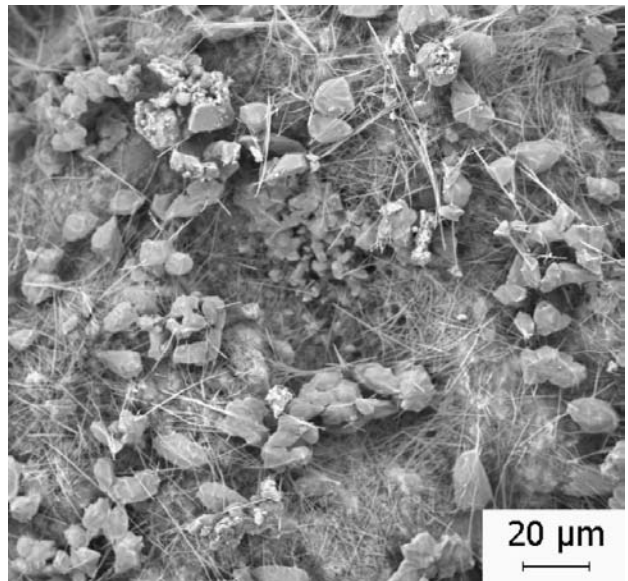


Figure 15. SEM micrograph of anhydrate crystals on the (L) samples (CPII-Z-32 cement/sand/5% grit) after 28 days of aging.

addition of grit to the mortar. The grit used in this study was high quality sand, but its surface contained ash from burnt oil, which tends to inhibit the nucleation and growth of anhydrate crystals in the material's structure.

4. Conclusions

This investigation demonstrated that microstructural and morphological studies are essential to gain a better understanding of the effect of solid industrial waste in mortar for construction applications. Of particular note was the marked difference between the compositions of the two Portland cements analyzed here. The large amount of inert

ash in CPII-Z-32 cement was found to be responsible for the lower mechanical strength and coarser microstructure of these samples than of those prepared with higher quality cement (CPI-S-32 cement).

The morphology of the bottom ash cement revealed smaller grain sizes than those of the cement powder. The morphology of the grit, in comparison to the sand, presented larger grain sizes, which did not, however, affect the material's microstructure.

Unlike the (Rs) matrix, the (Rz) matrix fracture surface micrographs showed a porous microstructure with a disordered anhydrite crystal growth. This was tentatively attributed to the large amount of inert ash in the cement, which inhibits the development of gel and, hence, the nucleation and ordered growth of anhydrite crystals. The microstructure of the (K) samples (10% bottom ash) showed less porosity and better anhydrite crystal distribution than that of the (Rz) matrix. The samples prepared with CPI-S-32 cement plus 5% bottom ash (J) presented a microstructure resembling that of the (Rs) matrix. The waste powder was homogeneously distributed in the matrix, which presented low porosity and well-developed anhydrite crystals. The CPII-Z-32 cement with 10% grit (L) showed less porosity than that of the above-mentioned (Rz) and (K) samples, with a good aggregate/gel interface. Another feature observed was the fewer anhydrite fibers present in the microstructure compared to the matrix (Rz) and the (K) cement/10% bottom ash sample (Fig. 15).

This study revealed that the composition and microstructure of bottom ash waste were similar to those of hydraulic binders, while the grit used here presented a composition and microstructure resembling those of sand, thus allowing it to be perfectly incorporated in mortars in place of sand.

Despite their good mechanical strength, it was found that fiber and dreg wastes are better suited for application as energy sources rather than as hydraulic binders.

Acknowledgements

The authors thank the Brazilian research funding institution CNPq for its financial support of this work, and Klabin Celucat S.A for supplying the raw materials used in this investigation.

References

1. Masuero, A.B.; Dal Molin, D.C.C.; Vilela, A.F. *Anais do 13º CBECIMAT*, CD-Rom, p. 4769, 1988.
2. Moura, W.A.; Dal Molin, D.C.C.; Vilela, A.F. *Anais do 13º CBECIMAT*, CD-Rom, p. 3403, 1988.
3. Teles, A.R.; Camargo, N.H.A. *Elaboração e Caracterização de Blocos para Construção Civil a Partir de Resíduos sólidos Industriais*, Relatório de Iniciação Científica, CNPq, p. 51, 1999.
4. Watanabe, A.P.; Nunes, J.J.; Rebello, L.; Moreno, M.A.; Mendes, J.M.M.; Buchler, P.M. *Anais do 38 Congresso Brasileiro de Cerâmica e 2 Encontro de Mineradores e Consumidores*, v. 2, p. 546, 1994.
5. NBR 5732 - *Cimento Portland Comum - Especificações*.
6. Bauer, L.A.F. *Materiais de Construção*, Livros Técnicos e Científicos Ltda, v. 1, 5ª ed., RJ, p. 71 e 79, 1987.
7. NBR 77211 - *Agregados para Concreto - Especificações*.
8. NBR 12821 - *Preparação de Concreto em Laboratório*.
9. NBR 7215 - *Cimento Portland - Determinação da Resistência à Compressão - Método de Ensaio*.
10. NBR 5738 - *Moldagem e cura de corpos de prova cilíndricos ou prismáticos de concreto*.
11. NBR 5739 - *Ensaio de compressão de corpos de prova cilíndricos de concreto*.